EMW

MET O 11 TECHNICAL NOTE NO. 63

A NOTE ON A LONGWAVE RADIATION SCHEME FOR THE 10-LEVEL MODEL

By F. R. Hayes

Introduction

In response to Octagon mean statistics which showed that the Octagon is heating up at a mean rate of about 2 degrees Centigrade/day, it was proposed to incorporate a radiation scheme at all levels in the 10-level model. At present, the only incorporation of radiative exchange is at the surface of the earth, where the solar flux and net long-wave radiation flux at the ground are computed from a regression formula, and modified according to the amounts of high, medium and low cloud present in the grid square. By incorporating a scheme for radiative transfer at all levels in the model, it is hoped that, not only will the mean statistics show a more realistic trend in the mean temperature, but that also differential heating and cooling, both in the vertical and the horizontal, will have beneficial effects on the prediction of convection, jet streams, development, etc. Long wave cooling in the free atmosphere may reach several times the mean value, while the presence of clouds drastically reduces the cooling within the cloud, but increases cooling from the top of the cloud. Thus cloudiness and radiative transfer interact, and horizontal variations in cloudiness may produce large variations in the heating or cooling by radiation.

The criteria for such a scheme are that it is physically realistic, simple to apply, and computationally viable. The last is by no means trivial, because of the vast complexity of the complete equation of radiative transfer in the atmosphere. Solution of these equations would require computing time many orders of magnitude larger than the actual forecast period. All forecasting models employ great simplification, and the scheme presented here is based on such formulae which are widely used and generally accepted.

Long waves ($0.7\,\mu m < \lambda < 4\,\mu m$) only are considered, since the heating due to other wavelengths is considered less important in the region of the atmosphere

FH 3B

covered. This is the waveband associated with water vapour absorption; ozone absorption, important in the stratosphere, is effective in the ultraviolet ($\lambda < 0.35\mu m$) and in the visual ($0.5\mu m < \lambda < 0.7\mu m$), and is not considered in this scheme. Carbon dioxide absorption is less significant than water vapour, and is also ignored.

The scheme is composed of two independent parts: terrestrial radiation and solar radiation heating. The former is responsible for the computation of fluxes of radiation due to atmospheric emission, and radiation from clouds and the earth's surface. The latter calculates the heating due to absorption of the solar ray on passing through the atmosphere. At present the radiation scheme and the surface exchanges scheme act independently, using different formulations. It would be wise, at some time in the future, to make the two formulations compatible, particularly as the radiation scheme is likely to give a more accurate estimate of the long-wave radiative transfer at the ground than a simple regression formula.

Both parts of the radiation scheme have points of similarity: they both operate on the same data, and use the same estimates of fractional cloud cover. Most important, they both employ the standard method of parameterising the variation of absorbing water vapour in the path of radiation, that of the corrected absorber amount, u. This single parameter is an equivalent water amount in an interval corresponding to the integrated true water amount in the interval. This absorber amount may be corrected for both pressure and temperature, but it is only the pressure corrected absorber amount which we consider here, for computational simplicity. It is defined by:

$$u(p_1, p_2) = \int_{p_1}^{p_2} \frac{r(p)}{g} \cdot \frac{p}{p^*} \, dp \qquad (1)$$

where p^* is a reference pressure (1013.25 mb) and $r(p)$ is the humidity mixing ratio at pressure p.

Terrestrial Radiation

Following the treatment of Rodgers (1969), the flux of terrestrial longwave radiation at any pressure level p may be expressed by two similar formulae, one for the upward flux, one for the downward flux.

$$F^{\uparrow}(p) = \int_{0}^{u(p_T,p)} B(u) \frac{d\epsilon^{\uparrow}(u)}{du} du + \left[1 - \epsilon^{\uparrow}(u(p_T,p))\right].\left[tT_T^{\uparrow} + (1-t)F_T^{\uparrow}\right] \qquad (2)$$

$$F^{\downarrow}(p) = \int_{0}^{u(p,p_B)} B(u) \frac{d\epsilon^{\downarrow}(u)}{du} du + \left[1 - \epsilon^{\downarrow}(u(p,p_B))\right].\left[tT_B^{\downarrow} + (1-t)F_B^{\downarrow}\right] \qquad (3)$$

where:

$\epsilon(u)$ is the atmospheric emissivity = $\dfrac{\text{radiation emitted by a layer}}{\text{radiation emitted by a black body at the same temperature}}$

$B(u)$ is the Planck function, integrated over all wavelengths = $\sigma T^4(u)$

p_T, p_B are model pressure levels corresponding to the nearest radiating surfaces below and above the level .

F_T, F_B are the fluxes of radiation emanating from the radiating surfaces at p_T and p_B.

tT_T, tT_B are the fluxes of transmitted radiation through cloud reaching levels p_T and p_B.

t is the cloud transmissivity (= 0.5 for cirrus or 0.0 for medium or low cloud).

The integrals in equations (2) and (3) are performed in steps corresponding to the absorber amount in each model layer in the interval (p_T, p) or (p, p_B), and the integrated Plank function B(u) is computed using the corresponding layer temperatures in the interval. In order to make computing more efficient, the emissivities are not computed by Rodgers' formulae, but from quartic polynomials fitted to his data.

Values of r above 350 mb are interpolated linearly from r_{350} to r_{100}, where $r_{100} = 0.002 g\ Kg^{-1}$, following Manabe & Müller (1961), who indicate that the frost point at 100 mb is 190°K irrespective of season or latitude.

The first term in each of the equations corresponds to the emission of the clear air, integrated between the level under consideration and the nearest black body, and the second term corresponds to the radiation from the nearest black body surface, together with a correction for absorption by the intervening clear atmosphere. The absorptivity is set as the complement of the emissivity and hence the factor $(1-\epsilon(u))$ is used. Two equations are needed because of the different emissivities involved when the radiation is from a higher to a lower pressure and vice versa.

Medium and low clouds are assumed to act as black bodies, and hence are perfect absorbers and emitters of radiation, thus F_T and F_B are computed from the integrated Planck function using the cloud surface temperature, when there is cloud below or above the level under consideration. Cirrus clouds are assumed to behave as grey bodies, with a transmissivity of 0.5. The emission of radiation from the surface of cirrus clouds is taken to be 0.5 times the black-body value. If there is no cloud below the level, F_T is taken to be the upward longwave radiation flux at the earth's surface. This is

$F_T = \sigma T_S^4$ over sea, T_S is the sea surface temperature

$F_T = F^{\downarrow}(1000) + L$, where L is the net longwave radiation

flux at the ground, given by the surface exchanges formulation. If there is no cloud above the level, F_B is set to zero. Finally, at levels inside the cloud, radiative equilibrium is assumed to exist, and

$$F^{\uparrow} = F^{\downarrow}$$

The application of this scheme to the 10-level model is quite simple. Firstly, the fractions of the grid square covered by low, medium and high cloud are computed using the same formulae as in the computation of surface exchanges (Gadd & Keers 1970). High cloud extends from 200-400 mb, medium from 400-700 mb, and low cloud from 700-900 mb, and is assumed to exist through the full depth of each layer. Maximum overlap of clouds is assumed, and the fraction of the grid square corresponding to each of the eight combinations of cloud, shown in Figure 1, is computed from the formulae:

$$f_o = 1 - \max (C_H, C_M, C_L)$$

$$f_1 = C_L - \max (C_H, C_M)$$

$$f_2 = C_M - \max (C_L, C_H)$$

$$f_3 = \min (C_M, C_L) - C_H \qquad (4)$$

$$f_4 = C_H - \max (C_M, C_L)$$

$$f_5 = \min (C_L, C_H) - C_M$$

$$f_6 = \min (C_H, C_M) - C_L$$

$$f_7 = \min (C_H, C_M, C_L)$$

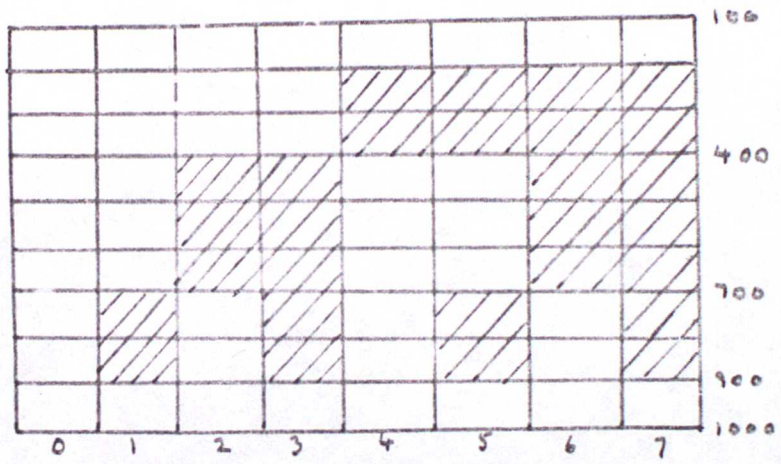

Fig 1

The f_i in (4) are subject to the constraints

$$f_i \geqslant 0$$

$$\sum_i f_i = 1 \qquad (5)$$

Inspection reveals that at most only four of the f_i are non-zero.

The upward and downward fluxes are computed for each cloud combination at the levels 100, 400, 700, 900 and 1000 mb, and are combined to give the net grid mean flux by weighting with the appropriate fraction for each cloud combination and summing:

$$\overline{F}(k) = \sum_{i=0}^{7} f_i \left(F_i^{\downarrow}(k) - F_i^{\uparrow}(k) \right) \quad ; \; k = 100, 400, 700, 900, 1000 \qquad (6)$$

The cooling rates are computed from:

$$\frac{d\overline{T}}{dt} = \frac{g}{Cp}\frac{d\overline{F}}{dp}, \qquad (7)$$

and are considered constant with pressure in each of the layers 100-400, 400-700, 700-900, 900-1000.

$$\begin{aligned}
\frac{\Delta T(j)}{\Delta t} &= \frac{g}{3Cp\Delta p}(\overline{F}(100)-\overline{F}(400)), \quad j = 150, 250, 350\\
\frac{\Delta T(j)}{\Delta t} &= \frac{g}{3Cp\Delta p}(\overline{F}(400)-\overline{F}(700)), \quad j = 450, 550, 650\\
\frac{\Delta T(j)}{\Delta t} &= \frac{g}{2Cp\Delta p}(\overline{F}(700)-\overline{F}(900)), \quad j = 750, 850\\
\frac{\Delta T(j)}{\Delta t} &= \frac{g}{Cp\Delta p}(\overline{F}(900)-\overline{F}(1000)), \quad j = 950
\end{aligned} \qquad (8)$$

Solar Radiation

The scheme for solar radiation heating is based on the Mintz-Arakawa scheme (see Arakawa, Katayama and Mintz, 1968), expanded to include ten levels and three cloud layers.

The insolation incident at the top of the atmosphere - taken to be 100 mb - is given by

$$S_o \sin\theta$$

where S_o is the solar constant, θ is the solar angle (see Gadd & Keers, 1970). The solar radiation is considered to consist of two parts ;a) $\lambda < 0.9\,\mu m$, in which Rayleigh scattering is significant, but water vapour is negligible and b) $\lambda > 0.9\,\mu m$, in which water absorption is significant, but scattering is slight. The portion of the solar radiation with $\lambda > 0.9\,\mu m$ is

$$S_o^A = 0.349\, S_o \sin\theta \qquad (9)$$

The radiation is subject to absorption in the atmosphere and reflection from clouds and the earth's surface, but, as in the terrestrial radiation scheme, no further absorption of the reflected radiation is computed.

Absorptivity is computed from the formula (Korb et al, 1956)

$$A(u) = 0.271(u)^{0.303} \quad (10)$$

In clear air, with no clouds above a pressure level, p, the relevant downward solar flux is

$$S^{\downarrow}(p) = S_o^A(1 - A(u(100,p).\mathrm{cosec}\,\theta)) \quad (11)$$

At the cloud top, a proportion R_c of the solar radiation flux is reflected, but the reflected ray is not further absorbed. Therefore, above the cloud

$$S^{\uparrow}(p) = S_o^A R_c(1 - A(u(100,p_T).\mathrm{cosec}\,\theta)) \quad (12)$$

where p_T is the pressure level of the cloud top.

Inside the cloud, multiple scattering by cloud droplets occurs, and this is incorporated into the formula, viz:

$$S^{\downarrow}(p) = S_o^A(1-R_c)(1 - A(u(100,p_T).\mathrm{cosec}\,\theta + 1.66\,u(p_T,p))) \quad (13)$$

Below cloud, the solar radiation is diffuse, and the same equation (13) is applied. Inside cloud, the absorber amount is derived from the saturation humidity mixing ratio in the layer.

The application of the scheme to the 10-level model is exactly similar to the terrestrial radiation scheme. Net solar fluxes for each cloud configuration are computed using equations (9)-(13), and the grid mean net solar flux computed from

$$\overline{S}(k) = \sum_{i=0}^{7} f_i(S_i^{\downarrow}(k) - S_i^{\uparrow}(k)); \; k = 100, 400, 700, 900, 1000 \quad (14)$$

Heating rates are computed in an analagous way to equation (8).

The cloud combination involving high and low cloud, but not medium cloud presents no problem: since the light is diffuse below the high cloud, equation (13) is applied at all levels below this level, whether in clear air or cloud.

Results

In order to test the performance of the radiation scheme in the 10-level model, some 16 octagon forecasts were run to 3 days, and one of these was run on to 6 days. Although the effects of the radiation scheme would be most visible in a 6 day forecast, there is considerable loss of accuracy after 3 or 4 days,

and it was felt that 3 day forecast runs presented an adequate compromise in which the forecast synoptic features were usually indentifiable with real ones, and in which the radiation scheme had sufficient time to produce significant changes (if any). In the event, certain of the changes due to the scheme were apparent well before 3 days. The 6-day forecast was run to verify the assumptions that changes would be larger than at 3 days, and also that the integration would remain stable.

Of the 16 forecast runs, 11 were run on successive days, from the 19th to 29th February 1976. The remainder were chosed at random from a rather limited range of summer forecasts, and covered the months of May to September in 1975. Synoptically, the summer forecasts provided a richer source of beneficial changes due to the radiation scheme, but the consecutive winter forecasts provided a better basis for statistical analysis, since 8 of the forecast initial fields furnished verification fields for the forecasts.

Statistical Analysis

In order to gain insight into the general behaviour of the radiation scheme, values of parameters averaged over the whole octagon forecast area, and over the two sets of winter and summer forecasts were considered. Figure 1 shows the development throughout the 72 hour forecast period of various mean parameters extracted from the winter set of forecasts. In all the figures a continuous line represents the forecasts with the radiation scheme included, and a dashed line, the forecasts without the scheme. Since most of the initial fields acted as verification fields for the forecast, there should be little change in the evolution of any particular parameter, such as is displayed in the 500-300 mb thicknesses. Departures from a constant value indicate the general trend of the forecast to warm up, cool down, etc. As can be seen from Figure 1, the general trend of the forecast without radiation was to increase both the 1000-500 mb and the 500-300 mb thickness values. The 1000 mb contour height had some small variation, and the corresponding trend of the 300 mb contour height, being the sum of the last three mentioned, was to increase by 5 Dm in 72 hours. This trend has led to unacceptable forecast root-mean-square errors of the 300 mb field. In contrast to this, the corresponding mean thickness in the forecast with radiation remained close to a

constant value, indicating the general cooling effect of the radiation scheme. However, the 1000 mb contour height now increased by 2 Dm in 72 hours, most of this change being apparent in the first 24 hours of the forecast. This corresponds to a general increase of mean surface pressure of 2.4 mb in 72 hours. Because of the consistent cooling due to the radiation, the 300 mb contour height increase is reduced to 2 Dm, a considerable improvement on the forecasts without radiation.

Figure 2 shows the corresponding diagrams for the 5 randomly chosen summer forecasts. Because of the smaller sample size, and the lack of verification statistics, less weight may be placed on these results than on the winter set. Nevertheless, the same general trends are discernable: the consistent cooling of the 1000-500 mb and 500-300 mb thicknesses, the poorer 1000 mb contour heights, and the imporved 300 mb contour heights. Because of the relative greater importance in summer of the compensating solar heating, the effect of inclusion of the radiation scheme is less marked in the statistical results. It is of interest to note that the 1000-500 mb thicknesses are cooled by rather too much by the radiation scheme, and the increase in the 1000 mb contour heights are not more marked in the first 24 hours as they were in the winter set.

Figure 3 shows the 72-hour temperature changes produced by the forecast with and without radiation, for both the winter and summer sets. They broadly confirm the impression of the radiation scheme imposing a cooling of 1.5°C in 72 hours at all levels in the model. In summer the cooling is less marked. Cooling is also less marked in the top and bottom layers. An exception to this is the rather large cooling in the bottom three layers during the summer forecasts. For most of the model layers, however, the 0-72 hour temperature changes are brought down nearer to zero.

The statistics show that, for the most part, the radiation scheme counteracts the current tendency of the 10-level model to heat up, and is of the right order to restore a general equilibrium in the heat energy cycle. However, two undesirable effects also emerge. Firstly, the apparent extra cooling of the lower layers in the summer forecasts. If this effect is real, and not a result of a poor sample, it is probably due to some deficiency in the treatment of low clouds in the solar part of the scheme, since the effect is not so noticeable in winter, and heating from the

sun is greatest in low clouds in the summer. The second effect is the general rise of pressure in the model. As will be shown later, this does not indicate a poorer synoptic forecast, but it does tend to fill the centres of depression by a few mb. It would be useful, therefore, if further research were to clarify the problem in these two areas.

Synoptic Analysis

Three forecasts are shown, to indicate features of the synoptic changes brought about by inclusion of the radiation scheme. These forecasts were chosen to indicate the longest changes observed in summer and in winter, and while one forecast shown is for T+6 days, the other two, representative of winter and summer are for T+48 hours. Generally, the further changes by T+72 hours were quite small, while the shorter forecast period gave better opportunity for verification with real features.

Figures 4-7 show the 48 hour forecasts from 00Z 21/2/76, together with verifying analyses. Both forecasts (Figures 4,5) verify with Figure 7, the initialised field at 00Z 23/2/76. However, the field from 12 hours prior to this time (Figure 6) is also included to illumine the development of a secondary Atlantic depression, marked 'P' on the charts (identified by this letter in the DWR charts). During the period of the forecast, Low P moved eastwards from Newfoundland, eventually becoming absorbed in the main Icelandic low before T+48. Thus, at the verification time, Low P had already lost its identity. At this time, a further embryonic development was taking place in mid-Atlantic. Both the forecasts with and without radiation appear to be 12 hours slow in the development of Low P, hence the need for Figure 6. Verifying the forecast development of Low P against the actual development, but without regard to the 12 hour timing error, it can be seen that the forecast with radiation produces a significant imporvement, particularly in the gradients of height, and corresponding increased surface winds. The central pressure is 4 mb deeper, and closer to the central pressure of Low P, when it was in this position. The timing error for both forecasts is identical. Note that this error is not consistent over the whole chart: the forecast depression over Newfoundland is well forecast by both schemes in position, but both are in equal error

in central pressure. The other most noticeable feature of the forecast was the rise of pressure. The statistics have shown that a general rise of about 2 mb in 72 hours is present, but this rise is not evenly distributed. Depressions are often affected by a rise of this magnitude, but not always, as has just been shown. In particular, anticyclones build pressure much more readily, by as much as 8 mb. In this forecast, the Scandinavian and Atlantic anticyclones have each been raised by about 4 mb in 48 hours. That this should be so is easily appreciated, since anticyclonic weather tends to reduce cloudiness, and thus enhance the local cooling of the atmosphere by radiation to space. The reduction of cloudiness also reduces the solar heating in this area. The cooling produces large-scale sinking motions, and the build up of the anticyclone.

The 6-day forecasts (Figures 8 and 9) have no verifying charts, since they were both so much in error that individual features were not identifyable. They do show, however, the extent to which the radiation scheme modified the forecast after 6 days. Most noticeable charges are: the depression west of Greenland - some 11 mb deeper, the Great Lakes depression - 3 mb deeper, and distinctly altered in shape, and the depression off the eastern seaboard of America - little different in central pressure, but very different in position and gradient of cortour height. Generally, anticyclonic central pressure is higher.

Finally, Figures 10-12 portray the 48 hour forecasts from 00Z 13/7/75, together with the verification at 00Z 15/7/75. Being a summer case, the general activity of the model is less than in winter, but changes due to the inclusion of radiation are greater. In 48 hours, the anticyclone off the eastern seaboard of America has been enhanced by 7 mb by the inclusion of the radiation scheme. A depression over Scotland also illustrates an interesting feature of the scheme. The central pressure of the depression is now 3 mb less deep than its counterpart in the forecast without radiation. However, because of the corresponding build-up of pressure in surrounding anticyclones, the gradient is much better forecast when radiation is included. In addition, the centre of the depression is some 400 km further on, and now positioned accurately. In this way, it is seen that the general rise in surface pressure, although undesirable is much less harmful to the forecast than the other changes are beneficial.

The remaining forecasts generally displayed the same characteristics as these, but with less noticeable changes. The depressions generally filled by a few mb, but with some exceptions. The anticyclones built, usually in the first 24 hours, by 4-6 mb, sometimes greater. This latter tendency usually improved the quality of the forecast by bringing high pressures closer to their actual value and by increasing the gradients of contour heights. The associated increase of wind also improved the mobility of some features.

A further feature of all forecasts was the considerable enhancement of rainfall. Accumulated rain, meaned over the whole grid was increased by 52 per cent in winter and 93 per cent in summer. Startling as these figures may seem, they represent a less important improvement that those already mentioned. Because of the large grid-length of the model, rainfall comes very close to being a sub grid-scale feature, and is correspondingly forecast to be very patchy in the model. Radiation in the forecast does help to join up the bands of otherwise patchy frontal rainfall, and this may be seen to be a useful improvement, but most of the additional rain falls in the tropical areas, and may even err to the extent of over-production. Taking an area including most of Europe and Scandinavia, the rainfall was increased by 32 per cent in winter and 65 per cent in summer.

Conclusions

This paper describes a longwave radiation scheme for use in the Meteorological Office 10-level model. It is founded on generally accepted principles of inclusion of certain parameterised radiative exchange processes deemed to be important to a Radiation scheme of this nature, ie relatively short-period numerical forecast. In particular, it includes the Mintz-Arakawa solar radiation scheme, modified to include 10 levels, with 3 cloud layers. Certain effects of the scheme (build-up of pressure in anticyclones) are noticeable quite early in the forecast (T+24 hours), and this would indicate its suitability for inclusion in the Rectangle version of the 10-level model. Other beneficial effects are the increase of gradient, particularly in depressions and the better development and movement of some depressions. Rainfall

is also enhanced, and frontal rainfall is delineated more clearly. The scheme Produces rather too much cooling in lower layers during the summer, and also the general level of pressure in the model is raised by about 2 mb in 72 hours. These last two do not appear to be serious deficiancies, however, and are more than compensated for by the other beneficial features of the scheme. Further research would, however, be clearly helpful towards eliminating these undesirable features.

References

Arakawa, A., Katayama, A. and Mintz, Y.	1968	Numerical Simulation of the General Circulation of the Atmosphere. Proc. WMO(IUGG) Symp. Nat. Wea. Prediction), Tokyo, 1968.
Gadd, A. J. and Keers, J. F.	1970	Surface exchanges of sensible and latent heat in a 10-level model atmosphere. Quart. Journal, 96, pp 297-308.
Korb, G., Michalowsky, J. and Möller, F.	1956	Investigation of the heat balance of the troposphere. AFCRL TN-56-881, 94 pp.
Manabe, S. and Müller, F.	1961	On the radiative equilibrium and heat balance of the atmosphere. Mon. Wea. Rev. 89, pp 503-532
Rodgers, C. D.	1967	The use of emissivity in atmospheric radiation calculations. Quart. Journal, 93, pp 43-54.

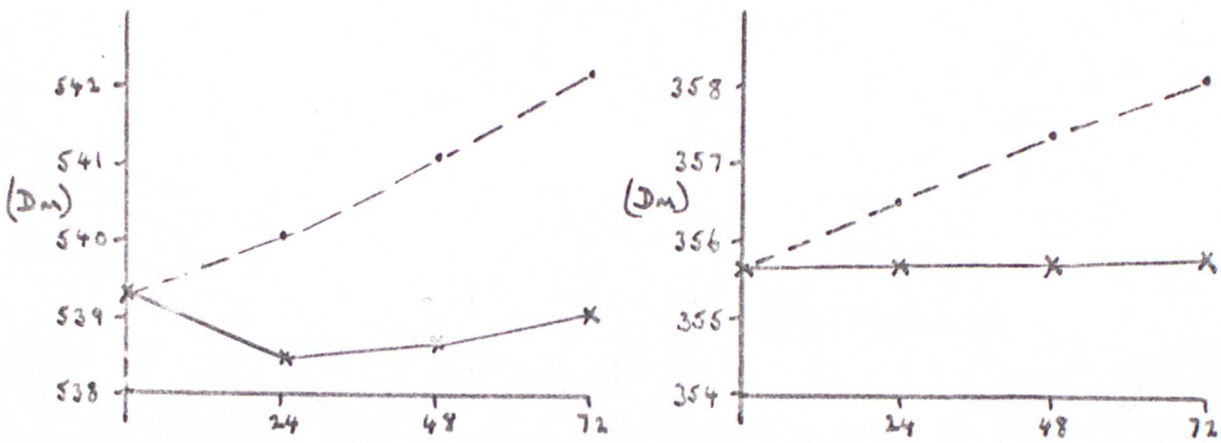

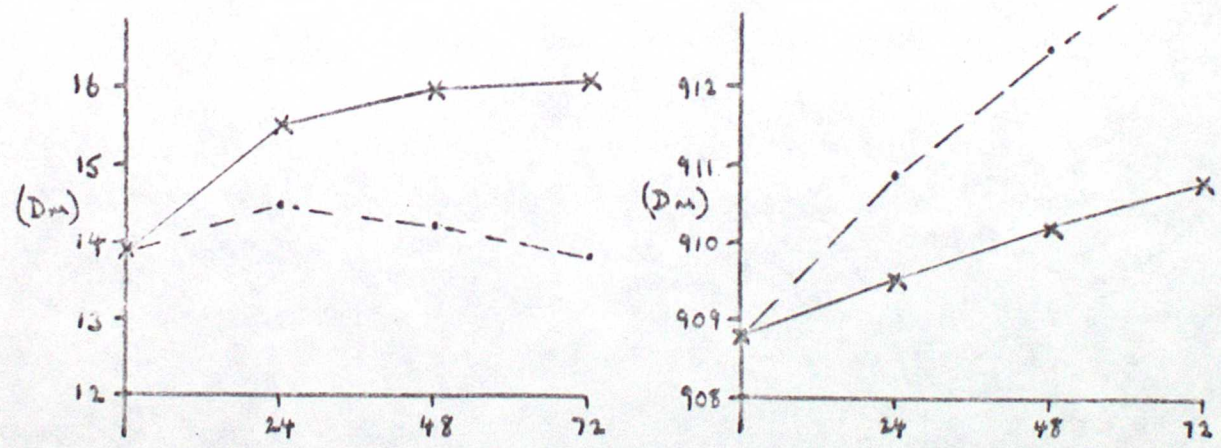

FIGURE 1.

11 WINTER CASES

MEANS OVER OCTAGON GRID AREA

·- - - -· WITHOUT RADIATION

×——× WITH RADIATION

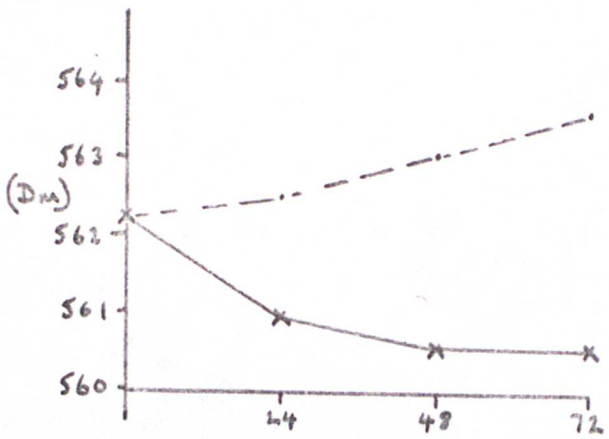

1000 - 500 mb THICKNESS

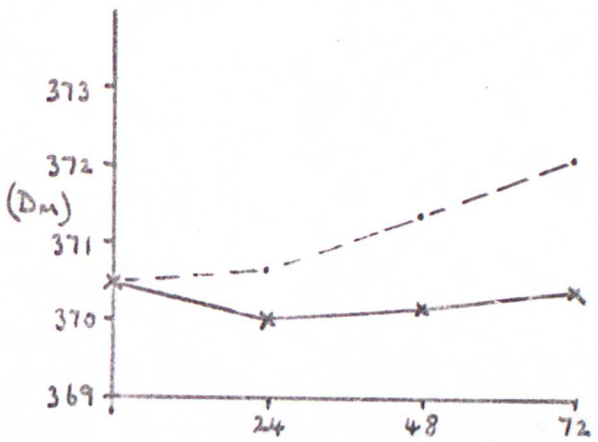

500-300 mb THICKNESS

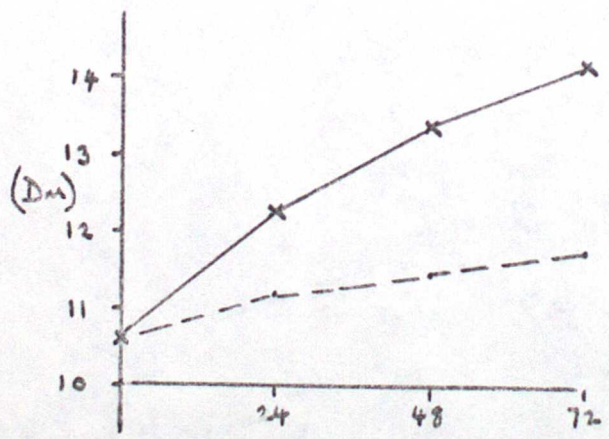

1000 mb CONTOUR HEIGHT

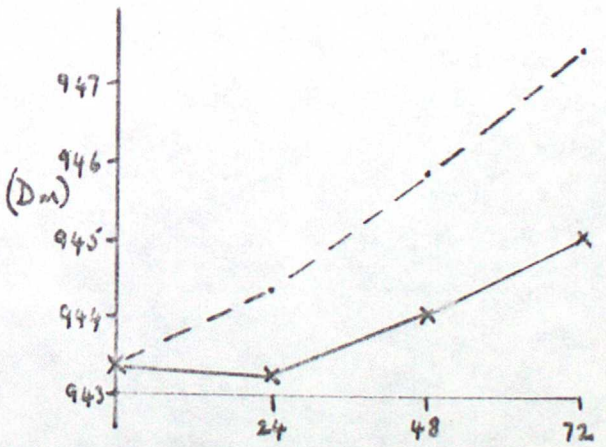

300 mb CONTOUR HEIGHT

FIGURE 2.

5 SUMMER CASES

MEANS OVER OCTAGON GRID AREA

·— — —· WITHOUT RADIATION

×——× WITH RADIATION

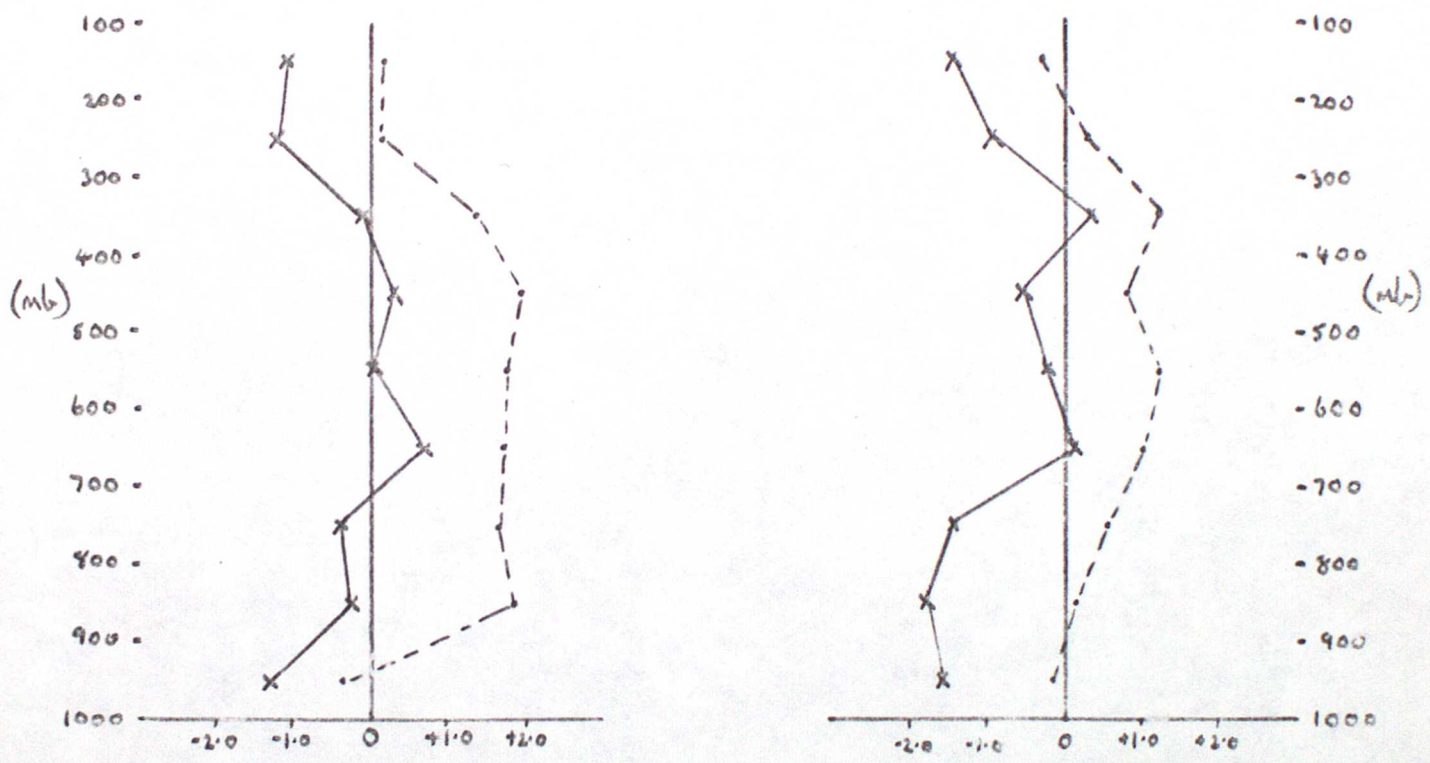

FIGURE 3.

MEANS OVER OCTAGON GRID AREA

•— — —• WITHOUT RADIATION

X——— X WITH RADIATION

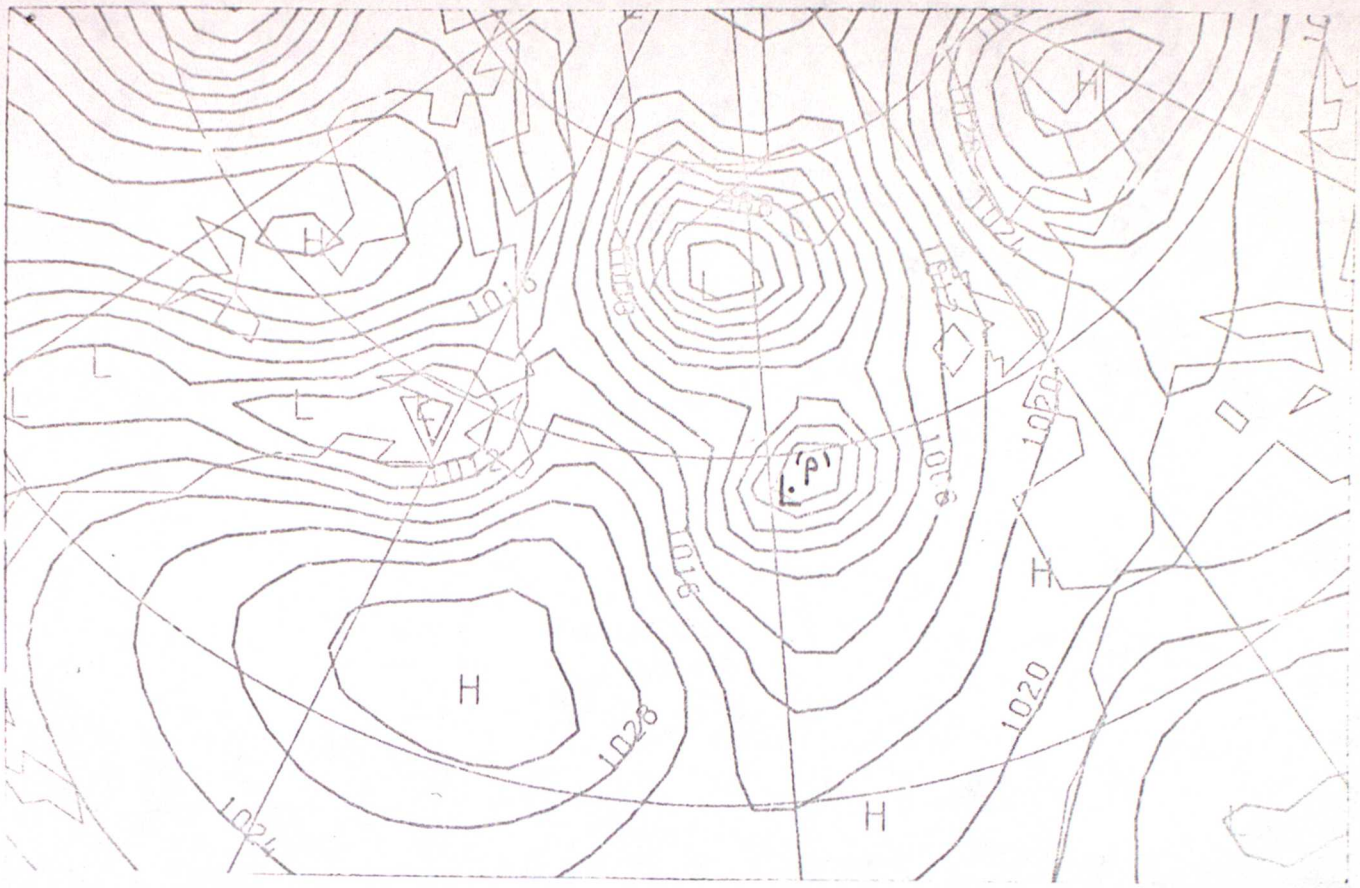

FIGURE 4

T+48hrs WITHOUT RADIATION. DATA TIME 00Z 21/2/76

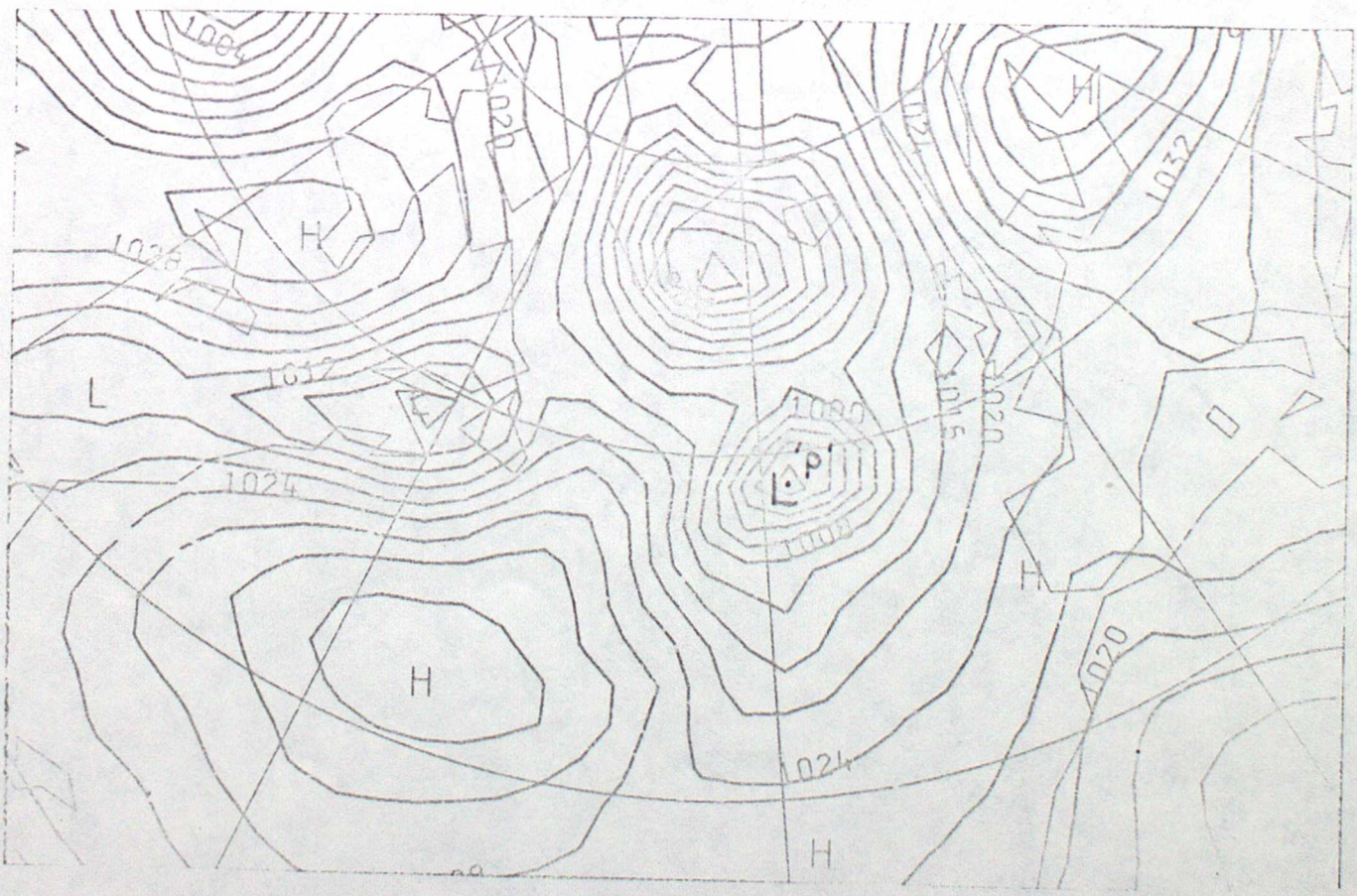

FIGURE 5

T+48hrs WITH RADIATION. DATA TIME 00Z 21/2/76

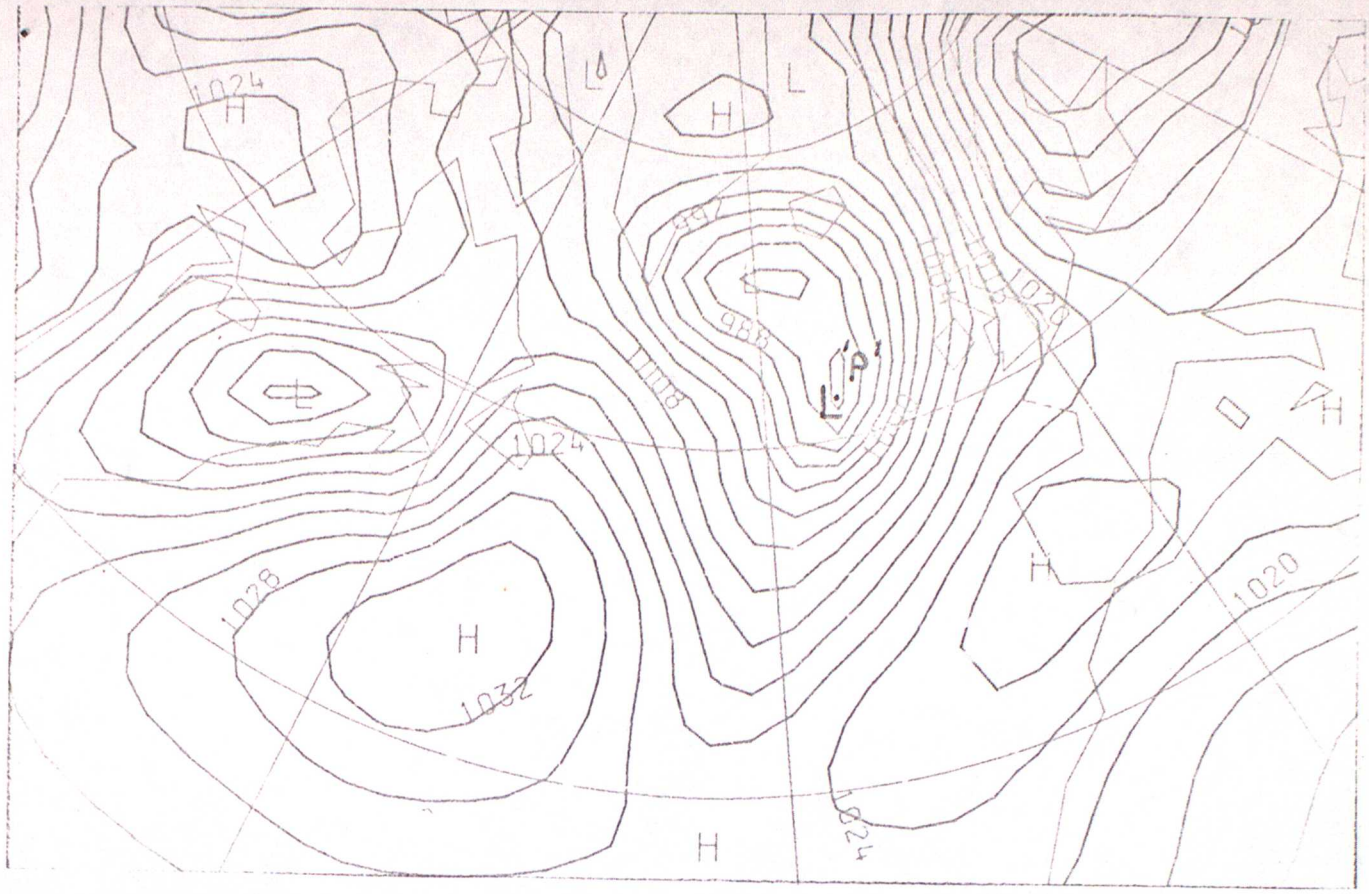

FIGURE 6

ANALYSIS : 12Z 22/2/76

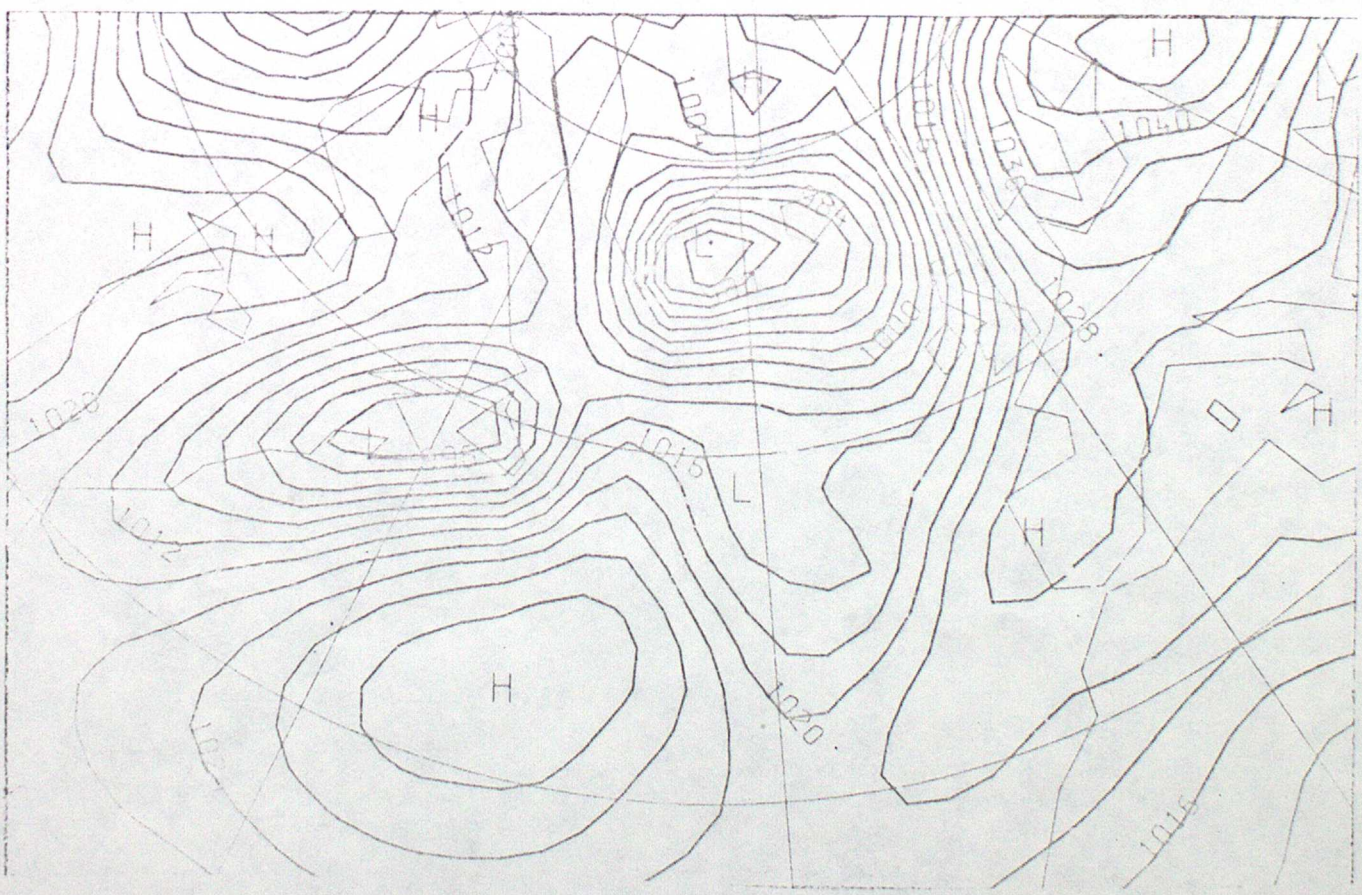

FIGURE 7

ANALYSIS : 00Z 23/2/76

FIGURE 8

T + 144 hrs WITHOUT RADIATION. DATA TIME: 00Z 25/2/76

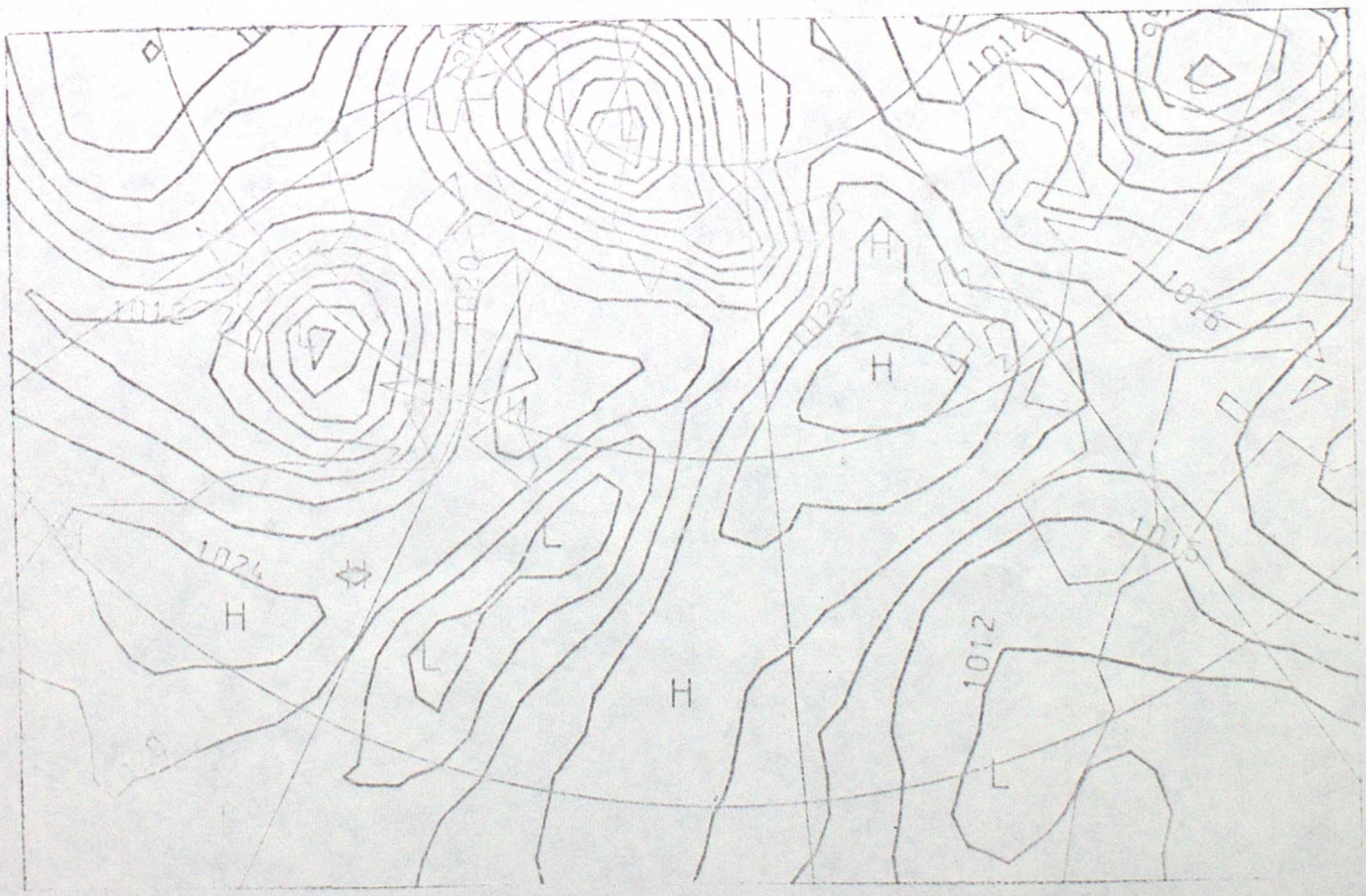

FIGURE 9.

T+144 hrs WITH RADIATION. DATA TIME: 00Z 25/2/76

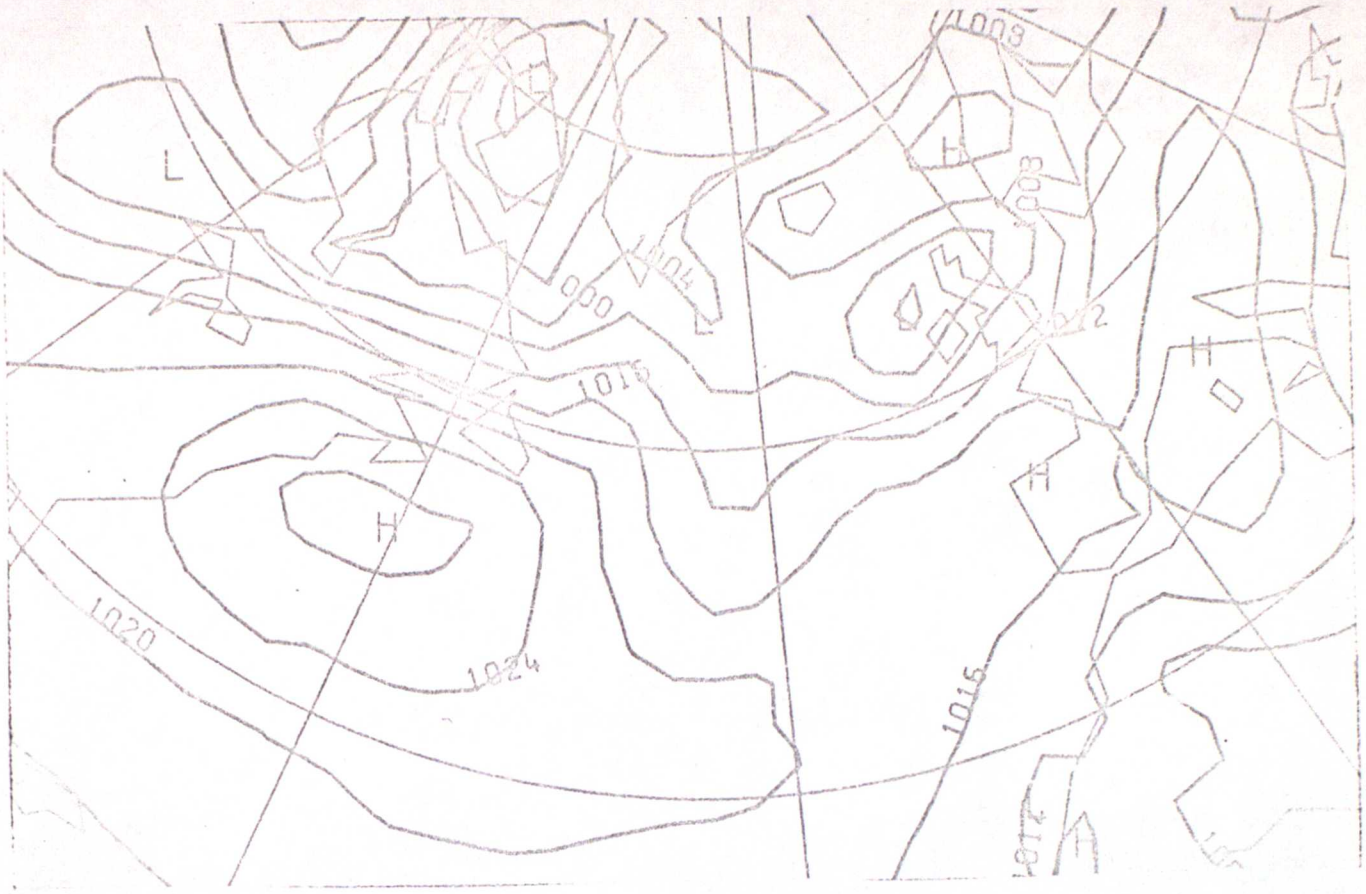

FIGURE 10.

T+48hrs WITHOUT RADIATION. DATA TIME: 00Z 13/7/75

FIGURE 11

T+48 hrs WITH RADIATION. DATA TIME: 00Z 13/7/75

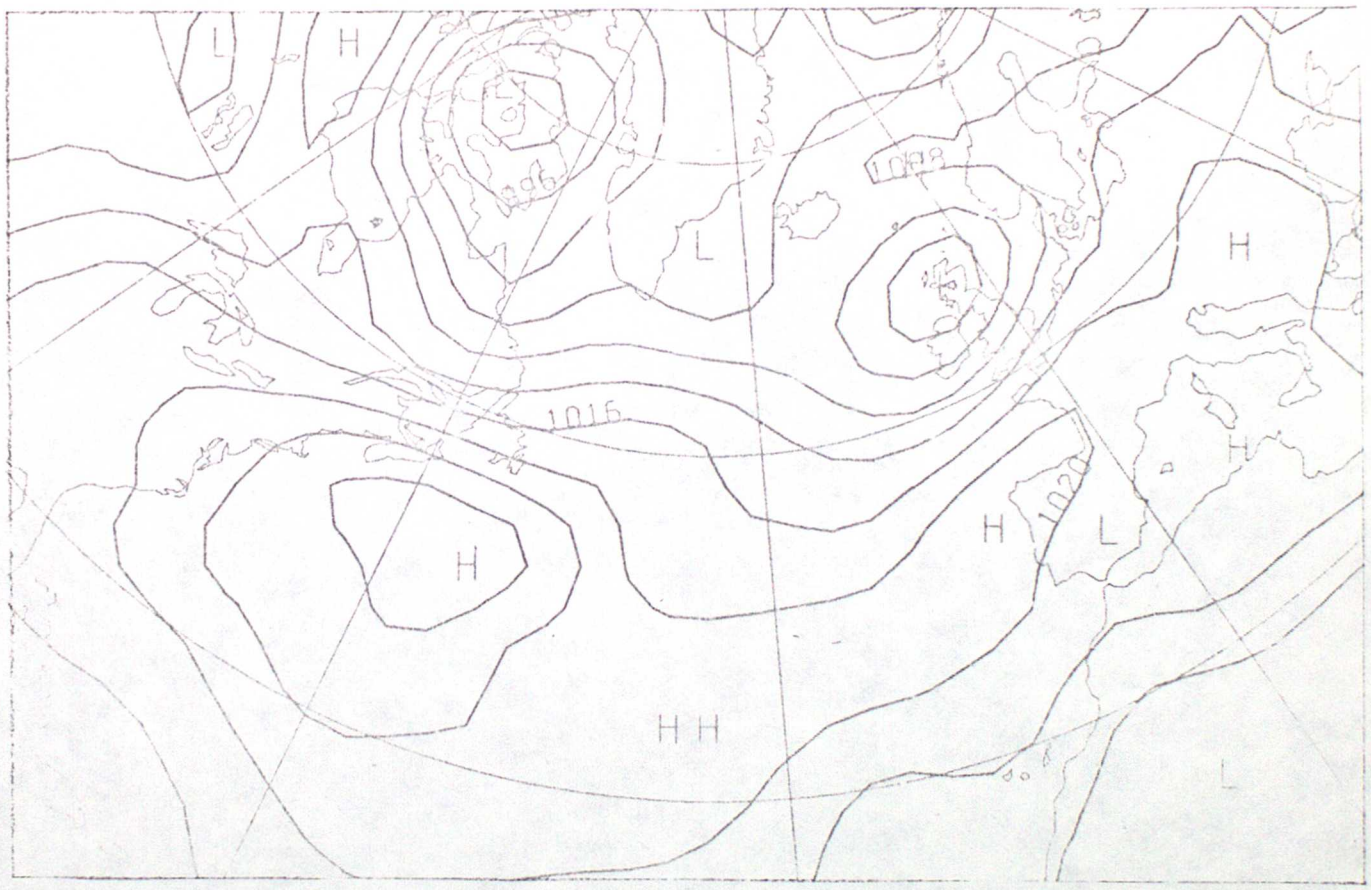

FIGURE 12.

ANALYSIS: 00Z 15/7/75